JACS
JOURNAL OF THE AMERICAN CHEMICAL SOCIETY
Article
pubs.acs.org/JACS

In Situ Catalyst Modification in Atom Transfer Radical Reactions with Ruthenium Benzylidene Complexes

Juneyoung Lee,[†] Jessica M. Grandner,[‡] Keary M. Engle,[†,§] K. N. Houk,[‡] and Robert H. Grubbs*[,†]

[†]Arnold and Mabel Beckman Laboratories of Chemical Synthesis, Division of Chemistry and Chemical Engineering, California Institute of Technology, Pasadena, California 91125, United States

[‡]Department of Chemistry and Biochemistry, University of California, Los Angeles, California 90095, United States

Supporting Information

ABSTRACT: Ruthenium benzylidene complexes are well-known as olefin metathesis catalysts. Several reports have demonstrated the ability of these catalysts to also facilitate atom transfer radical (ATR) reactions, such as atom transfer radical addition (ATRA) and atom transfer radical polymerization (ATRP). However, while the mechanism of olefin metathesis with ruthenium benzylidenes has been well-studied, the mechanism by which ruthenium benzylidenes promote ATR reactions remains unknown. To probe this question, we have analyzed seven different ruthenium benzylidene complexes for ATR reactivity. Kinetic studies by ^{1}H NMR revealed that ruthenium benzylidene complexes are rapidly converted into new ATRA-active, metathesis-inactive species under typical ATRA conditions. When ruthenium benzylidene complexes were activated prior to substrate addition, the resulting activated species exhibited enhanced kinetic reactivity in ATRA with no significant difference in overall product yield compared to the original complexes. Even at low temperature, where the original intact complexes did not catalyze the reaction, preactivated catalysts successfully reacted. Only the ruthenium benzylidene complexes that could be rapidly transformed into ATRA-active species could successfully catalyze ATRP, whereas other complexes preferred redox-initiated free radical polymerization. Kinetic measurements along with additional mechanistic and computational studies show that a metathesis-inactive ruthenium species, generated in situ from the ruthenium benzylidene complexes, is the active catalyst in ATR reactions. Based on data from ^{1}H, ^{13}C, and ^{31}P NMR spectroscopy and X-ray crystallography, we suspect that this ATRA-active species is a $Ru_xCl_y(PCy_3)_z$ complex.

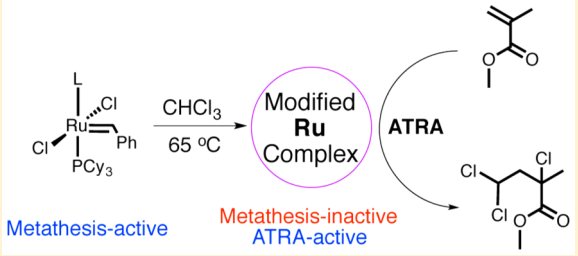

INTRODUCTION

Since the first report of ruthenium-based catalysts in atom transfer radical addition (ATRA, also called Kharasch addition)[1] and atom transfer radical polymerization (ATRP),[2] this area of research has attracted widespread interest.[3−14] Well-defined ruthenium benzylidene complexes, commonly used as olefin metathesis catalysts, have also been reported to catalyze ATRA and ATRP.[9,15−19] The ability of ruthenium benzylidene complexes to promote two reactions with such markedly different mechanisms has been utilized in various tandem reactions in which olefin metathesis and ATR reactions take place in one pot.[20−22]

Generally speaking, tandem catalysts, which catalyze multiple distinct reactions in one pot, are attractive synthetic tools that can simplify reaction procedures and reduce operational costs. An improved understanding of their mechanism can enable further catalyst development toward new applications. Among the many tandem catalysts that have been reported,[23] ruthenium benzylidene complexes have been a topic of interest to our research laboratory. For example, our group has reported ring opening metathesis polymerization (ROMP)-ATRP tandem catalysis for the preparation of block copolymers of 1,5-cyclooctadiene and methyl methacrylate (MMA).[20] Since the ROMP process was more rapid than ATRP, excess PCy_3 was added to the reaction and low-strain cycloolefins were employed to suppress the rate of ROMP. Using low-strain cycloolefins and excess phosphine, the rate of ROMP was suppressed to roughly the same rate as ATRP, allowing for productive tandem catalysis. While the mechanism by which ruthenium benzylidenes initiate and catalyze olefin metathesis has been studied in great detail, little is known regarding the mechanism of ATR reactions promoted by these complexes.

Herein, we present our findings regarding the mechanism of these reactions. We have performed kinetic studies of ATRA using various ruthenium benzylidene complexes. Under common ATRA conditions, these complexes were found to rapidly consume the alkene starting material, but not all of them promoted formation of the desired ATRA product. Our experimental results are consistent with a decomposed ruthenium species, rather than the ruthenium benzylidene, as the active ATRA catalyst in this system. These ATRA-active ruthenium complexes were further found to be inactive in olefin metathesis. We have attempted to identify the new ATRA-active ruthenium species. To do this, we employed NMR spectroscopy and X-ray crystallography. Finally, when this

Received: April 12, 2016
Published: May 17, 2016

DOI: 10.1021/jacs.6b03767
J. Am. Chem. Soc. 2016, 138, 7171−7177

collection of ruthenium benzylidene complexes were tested in ATRP, we found that only the complexes that formed highly reactive ATRA catalysts were able to perform controlled polymerization, rather than redox-initiated free radical polymerization.

EXPERIMENTAL SECTION

Materials and Analytical Techniques. All reactions were carried out in dry vials with PTFE-faced silicone septa under an argon (Ar) atmosphere or in a Vacuum Atmospheres Glovebox under a nitrogen atmosphere, as specified. All solvents and reagents were purchased from Sigma-Aldrich and used without further purification unless otherwise noted. Fresh ampules of $CDCl_3$ (Sigma-Aldrich) were used in decomposition experiments of the ruthenium benzylidene catalysts. Complexes **1**, **2**, **3**, **6**, and **7** were obtained from Materia, Inc. Complexes **4** and **5** were prepared from **2** and **3**, respectively, following literature procedures.[24,25] ^{1}H NMR spectra were recorded on one of the following instruments: Varian Mercury (300 MHz), Varian Inova (500 MHz), or Bruker Ascend with Prodigy broadband cryoprobe (400 MHz). Gel permeation chromatography (GPC) was conducted on two Agilent PLgel 10 μm MIXED-BLS 300 mm × 7.5 mm columns with Agilent P260 series pump and autosampler with Wyatt Dawn Heleos-II multiangle static light scattering detector and Optilab T-rEX differential refractive index detector with THF as an eluent.

General Procedure for ATRA Catalyzed by Ruthenium Benzylidene Complexes. To an 8 mL vial with silicone septum cap equipped with a magnetic stir bar, complex **1** (62 mg, 0.75×10^{-1} mmol), MMA (106.84 μL, 9.99×10^{-1} mmol), and $CHCl_3$ (0.8 mL. 9.98 mmol) were added. Anisole (10 μL, 9.20×10^{-2} mmol) was added as an internal standard. The solution was degassed with Ar (g) for 10 min, and the reaction was initialized by immersing the reaction vessel into an oil bath preheated to the specified temperature (65 or 40 °C). The reaction was kept under Ar (g), and aliquots were removed at predetermined time points and analyzed by ^{1}H NMR to monitor reaction progress over time. After 2 h, the solution was precipitated into petroleum ether and filtered to remove precipitated catalyst. Solvent and unreacted MMA were removed using a rotary evaporator. The yield of the product was calculated based on integration of ^{1}H NMR resonances at 6.01 ppm ($-CCl_2\mathbf{H}$ from the product) and 1.84 ppm ($-C\mathbf{H}_3$ from the product and byproducts). All of the ATRA reactions in this paper were performed following this general procedure using the same molar ratio of [catalyst]: [MMA]: [$CHCl_3$].

Decomposition Study of Ruthenium Benzylidene Complexes. Inside the glovebox, an NMR tube was charged with the ruthenium complex and $CDCl_3$ in the same molar ratio as specified in the general ATRA procedure. The NMR tube was capped with a septum, removed from the glovebox, and heated to 65 °C. ^{1}H NMR spectra were collected at predetermined time points, and the integral of the benzylidene resonance (16−20 ppm, ^{1}H) was plotted as a function of time.

General Procedure for ATRA Catalyzed by Activated Ruthenium Complexes. To an 8 mL vial with silicone septum cap equipped with a magnetic stir bar, complex **1** (62 mg, 0.75×10^{-1} mmol), anisole (10 μL, 9.20×10^{-2} mmol), and $CHCl_3$ (0.8 mL, 9.98 mmol) were added. The solution was degassed with Ar (g) for 10 min and then heated to 65 °C, until the benzylidene ^{1}H NMR resonance had completely disappeared. The reaction vessel was allowed to cool to room temperature, and freshly degassed MMA (106.84 μL, 9.99×10^{-1}mmol) was added to the solution. The reaction was initialized by immersing the reaction vessel into an oil bath preheated to the specified temperature (65 or 40 °C) and was held under an Ar (g) atmosphere Aliquots were removed at predetermined time points and analyzed by ^{1}H NMR to monitor reaction progress over time. All of the ATRA reactions in this report with preactivated ruthenium benzylidene complexes were performed following this general procedure using identical concentrations.

General Procedure for ATRA Catalyzed by Ruthenium Benzylidene Complexes with 5 equiv of PCy_3. To an 8 mL vial with silicone septum cap equipped with a magnetic stir bar, complex **1** (62 mg, 7.53×10^{-2} mmol), MMA (106.84 μL, 9.99×10^{-1}mmol), anisole (10 μL, 9.20×10^{-2} mmol), and $CHCl_3$ (0.8 mL, 9.98 mmol) were added. PCy_3 (105.64 mg, 3.77×10^{-1} mmol) was then added, and the solution was degassed with Ar (g) for 10 min. The reaction was initialized by immersing the reaction vessel into an oil bath preheated to 65 °C and was held under an Ar (g) atmosphere. Aliquots were removed at predetermined time points and analyzed by ^{1}H NMR to monitor reaction progress over time. Experiments with **2** and **3** were performed following this general procedure using identical concentrations and reaction conditions.

RCM Catalyzed by 3 and Benzylidene-Decomposed (ATRA-Activated) 3. The reaction was performed following a literature procedure.[26] Complex **3** (7.47 mg, 8.01×10^{-3} mmol) was dissolved in degassed $CDCl_3$ (0.75 mL). For reactions catalyzed by decomposed **3**, the solution was then pretreated at 65 °C until the indicated level of benzylidene decay (as monitored by ^{1}H NMR) was observed. The catalyst solution was cooled to room temperature, and diethyl diallylmalonate (19.3 μL, 7.98×10^{-2} mmol) was added. The reaction mixture was brought to a temperature of 30 °C for 1 h, after which point an ^{1}H NMR spectrum was collected to calculate olefin conversion.

Crystallization of ATRA-Activated 1 with Bipy. Complex **1** (62 mg, 0.75×10^{-1} mmol) was dissolved into 0.8 mL of $CHCl_3$ (0.8 mL. 9.98 mmol) and was activated by heating at 65 °C until complete decay of the benzylidene peak in the ^{1}H NMR spectrum was observed. The solvent was removed under vacuum, and the resulting powder was redissolved in a minimal amount of DCM, prior to addition of bipy (58.83 mg, 0.38 mmol). Pentane was slowly added to make a layer above the DCM, and the solution was allowed to stand unperturbed at room temperature until crystals of the complex formed.

ATRA Catalyzed by Ru(III)Cl_3 and PCy_3 Complex. MeOH (0.8 mL) was added to Ru(III)Cl_3 (15.54 mg, 0.75×10^{-1} mmol) and PCy_3 (42.02 mg, 1.50×10^{-1} mmol), and the reaction mixture was heated to reflux overnight. The solvent was removed under vacuum. Benzene was added, and the solution was filtered through glass pipet with kimwipe plug. The filterate was again concentrated under vacuum to give a dried powder. To this solid, were added MMA (106.84 μL, 9.99×10^{-1} mmol) and 0.8 mL of $CHCl_3$ (0.8 mL. 9.98 mmol), followed by anisole (10 μL, 9.20×10^{-2} mmol) as an internal standard. The solution was degassed with Ar (g) for 10 min, and the reaction was initialized by immersing the reaction vessel into an oil bath preheated to 65 °C.

ATRP Catalyzed by Ruthenium Benzylidene Complexes. To an 8 mL vial with silicone septum cap equipped with a magnetic stir bar, ethyl α-bromoisobutyrate (10 μL, 6.81×10^{-5} mmol), MMA (1.46 mL, 1.36×10^{-2} mmol), and complex **1** (56.07 mg, 6.81×10^{-5} mmol) were added. Toluene (681 μL) and anisole (10 μL) were added as the solvent and internal standard, respectively. The solution was degassed with Ar (g) for 10 min, and the reaction was initialized by immersing the reaction vessel into an oil bath preheated to 85 °C. Aliquots were removed at predetermined time points and analyzed by ^{1}H NMR and GPC to monitor, MMA conversion M_n, and dispersity ($Đ$) over time. All of the ATRP reactions in this report were performed following this same general procedure under identical reaction conditions.

RESULTS AND DISCUSSION

This investigation was commenced by examining reaction kinetics of ATRA with a series of ruthenium benzylidenes commonly employed in olefin metathesis (Chart 1). All of these complexes have been previously reported to catalyze olefin metathesis, and **1** has been shown to be effective in ATR reactions.[9,19]

For ATRA, methyl methacrylate (MMA) was employed as a model substrate due to its well-established reactivity in ATRA and ATRP. Chloroform ($CHCl_3$) was chosen as the coupling partner and reaction solvent since ATRA using this halogen

DOI: 10.1021/jacs.6b03767
J. Am. Chem. Soc. 2016, 138, 7171−7177

Chart 1. Ruthenium Benzylidene Complexes

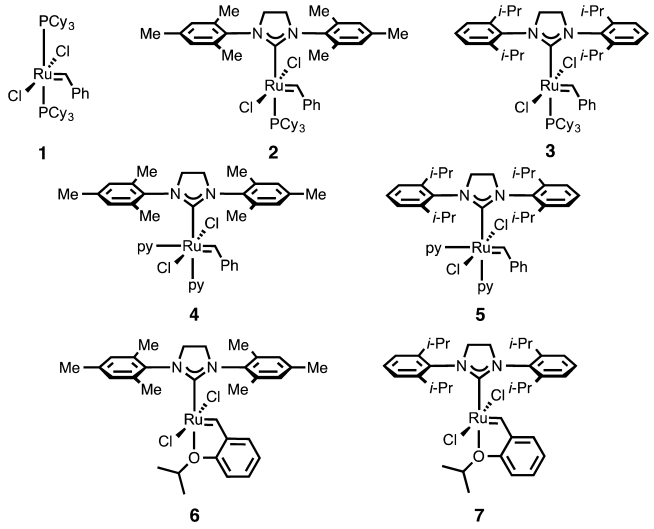

donor has been studied extensively (Scheme 1). Reactions with all of the complexes shown in Chart 1 were monitored over 2 h by measuring the MMA conversion at predetermined time points by ^{1}H NMR spectroscopy (Table 1).

Scheme 1. ATRA of MMA Catalyzed by Ruthenium Benzylidenes or Activated Ruthenium Complexes

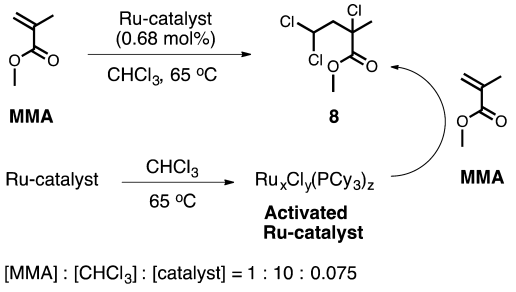

By monitoring MMA conversion over reaction time (Figure 1a and Table 1), it was found that five out of seven ruthenium benzylidene catalysts in the study led to consumption of MMA. Complexes **6** and **7** were found to be unreactive in ATRA. Complex **3** containing a SIPr ligand was the most active, followed in order by **1**, **4**, **2**, and **5**. The final yield of the desired product **8** was generally higher with faster ATRA catalysts. For example, with complexes **1** and **3**, >99% of consumed MMA was converted to ATRA product, whereas greater discrepancies between MMA conversion and product yield were observed with **2**, **4**, and **5**. In these cases, MMA may have been consumed in undesired oligomerization/polymerization, a well-known side reaction of ATRA. Notably, no relationship between metathesis activity (or metathesis initiation rate) and ATR rate was observed within this series.

Density functional theory (DFT) calculations were performed assuming a general mechanistic paradigm involving inner-sphere electron transfer from an intact ruthenium benzylidene moiety to homolyze the carbon–halogen bond (Figure S1). However, predicted relative catalyst activities from computed ΔG_{rxn} for this reaction with complexes **1**–**7** were not in agreement with the empirically observed reactivity trend. Additionally, the ΔG_{rxn} values for the halogen abstraction step with most complexes were too endergonic for effective catalysis.

Table 1. MMA Conversion and Product Yield of ATRA (2 h) with Different Ruthenium Benzylidene Complexes

entry	catalyst	T (°C)	MMA conv (%)[a]	yield for **8** (%)[b]
1	**1**	65	89	89
2	**2**	65	45	7
3	**3**	65	95	94
4	**4**	65	79	61
5	**5**	65	17	~0
6	**6**	65	~0	~0
7	**7**	65	~0	~0
8	activated **1**	65	97	86
9	activated **3**	65	99	93
10	activated **4**	65	86	68
11	**1**	40	20	~1
12	activated **1**	40	41	28
13	**3**	40	32	~2
14	activated **3**	40	85	70
15	**1** + 5 equiv PCy_3	65	67	16
16	**2** + 5 equiv PCy_3	65	40	~0
17	**3** + 5 equiv PCy_3	65	69	~2

[a]MMA conversion was calculated from ^{1}H NMR integration using anisole as an internal standard. [b]Product yield was calculated from ^{1}H NMR integration, after first removing the ruthenium catalyst by precipitation into petroleum ether.

This inconsistency prompted us to consider the stability of complexes **1**–**7** under the reaction conditions.

Solutions of each complex in $CDCl_3$ without MMA were prepared at the same concentration used in the ATRA experiments. The diagnostic benzylidene proton peak was monitored by ^{1}H NMR (16–20 ppm) over time at the reaction temperature (65 °C). Most of the catalysts were unstable in $CDCl_3$, as evidenced by the disappearance of the benzylidene peak and appearance of new proton resonances far upfield of the benzylidene region. Complexes **6** and **7** were stable for >4 h under these conditions (Figure 1b, Figures S2–S12). This decomposition process was found to be highly temperature- and solvent-dependent. For example, with catalyst **4**, no appreciable benzylidene decay was observed at a slightly reduced temperature of 55 °C for over 4 h. Complex **3** showed rapid benzylidene decay in $CDCl_3$ but did not show any benzylidene decay in C_6D_6 until subsequent addition of an alkyl halide (Figure 1c). This indicates that the alkyl halide triggers benzylidene decomposition. Furthermore, complex **3** exhibited a nearly identical benzylidene decay profile in $CDCl_3$ containing added K_2CO_3. These results are consistent with the alkyl halide, rather than heat or trace HCl, as the component that drives benzylidene decomposition. Strikingly, the order of benzylidene decay rate in these stoichiometric experiments was the same order as MMA conversion in catalytic ATRA (Figures 1a and b). The correlation between benzylidene decay rate and ATRA rate prompted us to examine the extent to which the newly formed ruthenium species are active participants in ATRA reactions.

To this end, the reactivity of the benzylidene-decomposed ruthenium species, formed from pretreatment of **1**, **3**, and **4** in $CHCl_3$, was investigated. First, solutions of these catalysts in $CHCl_3$ were heated at 65 °C under Ar (g) in the absence of MMA until no benzylidene peak was observed in the ^{1}H NMR spectrum. MMA was added, and reaction progress was monitored (Scheme 1). As shown in Table 1 and Figure 2a, the activated ruthenium complexes demonstrated faster rates,

DOI: 10.1021/jacs.6b03767
J. Am. Chem. Soc. 2016, 138, 7171–7177

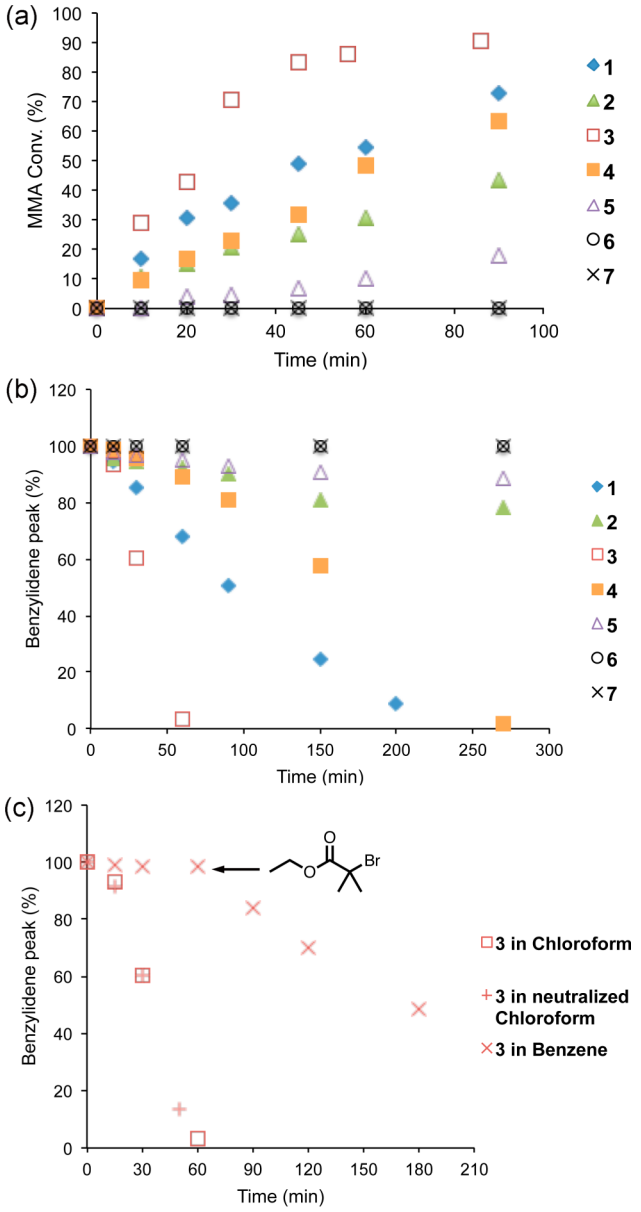

Figure 1. Rate profiles of (a) ATRA promoted by ruthenium benzylidene complexes. Reaction conditions as in Scheme 1. (b) Benzylidene ^{1}H NMR resonance decay of complexes **1**–**7** over time. Reaction conditions as in Scheme 1 in the absence of MMA. (c) Benzylidene ^{1}H NMR resonance decay of complex **3** in $CDCl_3$, neutralized $CDCl_3$, and C_6D_6 with addition of ethyl α-bromoisobutyrate after 1 h. In the neutralized experiment, excess K_2CO_3 solid was added to a freshly degassed $CDCl_3$ solution, and the resulting heterogeneous mixture was shaken vigorously prior to heating.

providing equally high yield of the ATRA product. Given the pronounced temperature dependence of the stoichiometric benzylidene decay reactions, we next sought to determine the temperature dependence of ATRA reactivity. When ATRA reactions were run with **1** and **3** at 40 °C, where no benzylidene decay was observed, MMA consumption proceeded slowly and only trace product formation was observed. In contrast, preactivated, benzylidene-decayed **1** and **3** exhibited faster rate and provided greater product yields, even at 40 °C (Table 1).

The data shown above indicate a reaction pathway for ATRA in which the ruthenium benzylidene is converted into one or

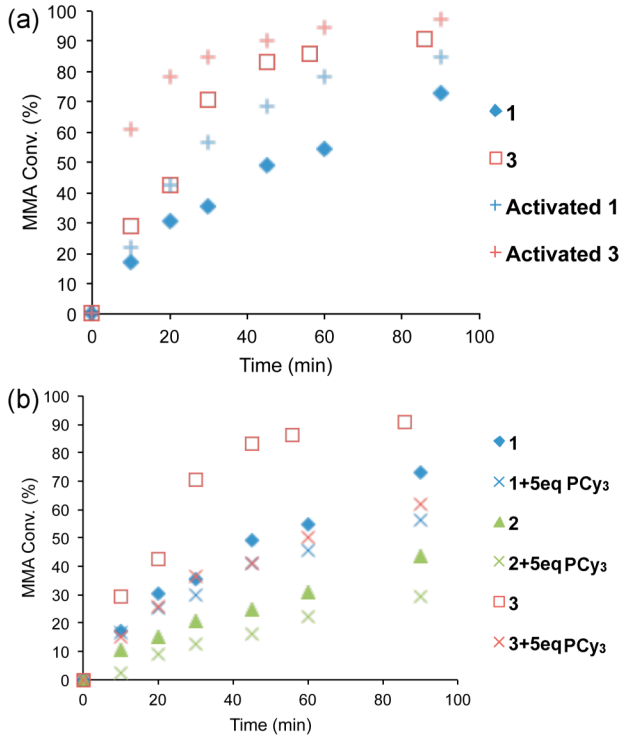

Figure 2. (a) Kinetic study of ATRA of MMA catalyzed by **1**, **3**, and their activated analogues. (b) Effect of adding PCy_3 (5 equiv) to ATRA catalyzed by **1**, **2**, and **3**. Reaction condition same as in Scheme 1.

more new ATRA-active ruthenium species under ATRA conditions. When activated, the new species exhibit superior reactivity in ATRA compared to the parent complexes, even at lower temperature. As is typical in ATR reactions, trials performed under our standard conditions were inhibited by O_2. Consistent with this observation, the newly formed ruthenium species were found to be air-sensitive and were unreactive in ATRA after exposure to air.

The effect of excess phosphine ligand in catalytic ATRA was also studied. The addition of tricyclohexylphosphine (PCy_3, 5 equiv relative to catalyst) to solutions of the complexes altered the benzylidene decomposition trends (Figure S13). With complexes **1** and **2**, the presence of additional PCy_3 increased the rate of benzylidene decay. However, complex **3** showed slower decay than **1** and **2** under the same conditions. The origins of these effects are still under investigation. The rates of catalytic ATRA reactions with additional PCy_3 using **1** and **2** were slightly inhibited by excess PCy_3. The reaction with **3** became substantially slower, and the overall product yield was significantly reduced in all cases (Table 1 and Figure 2b).

The identity of the in situ generated ruthenium species was explored further. Complex **3** was decomposed in $CDCl_3$ to 40% completion and 100% completion (as measured by benzylidene ^{1}H NMR signal). It was found that an ATRA-activated sample of **3** with completely decayed benzylidene was inactive in ring-closing metathesis (RCM) of diethyl diallylmalonate (**9**), a highly reactive RCM substrate with complexes **1**–**7** (Scheme 2). In contrast, samples of untreated **3** and 40%-benzylidene-decayed **3** catalyzed RCM with **9**, providing 100% conversion to **10** after 1 h. These results, in conjunction with the ^{1}H NMR data, prove that the ATRA-active ruthenium species does not contain a benzylidene/alkylidene moiety.

DOI: 10.1021/jacs.6b03767
J. Am. Chem. Soc. 2016, 138, 7171–7177

Scheme 2. RCM Catalyzed by 3 and Benzylidene-Decomposed ATRA-Activated 3

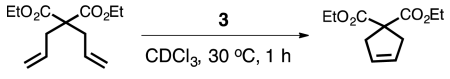

9 10

Catalyst	Conversion (%)
3	100
40% decomposed **3**	100
100% decomposed **3**	0

To gain more information regarding the structure of the ATRA-active species, we next turned to NMR spectroscopy and X-ray crystallography. As discussed above, upon decomposition of complexes **1** and **3** in $CDCl_3$ at 65 °C, the ^{1}H and ^{13}C NMR spectra revealed that the benzylidene moiety had fully dissociated. In the ^{31}P NMR spectra of ATRA-activated **1** and **3**, a substantial downfield shift of the major phosphine resonance was observed. In both cases, a major phosphine resonance at 108.10 ppm appeared upon decomposition (Figures S4 and S8). This peak is in an unusual region of the ^{31}P spectrum, and we suspect that it could represent the corresponding dichlorophosphonium salt.[27] The ^{31}P NMR results along with the data from excess PCy_3 experiments shown above (Table 1 and Figure 2b) with **1** and **3**, are consistent with a mechanism in which PCy_3 is partially or fully dissociated from the ruthenium center in the active form of the catalysts.

In addition to NMR spectroscopy, we have attempted to obtain single crystals of ATRA-activated ruthenium complexes **1** and **3** that would be suitable for X-ray diffraction. Despite numerous attempts, we were unable to grow suitable crystals directly from the decomposed solutions. However, after extensive experimentation we found that the addition of 2,2′-bipyridine (bipy, 5 equiv) to a solution of ATRA-activated **1** led to formation of a new species, $Ru(II)Cl(PCy_3)(bipy)_2Cl^-$, which we were able to crystallize and characterize by X-ray diffraction (Figure 3). Interestingly preliminary X-ray crystal structure data of the analogous experiment with activated **3** allowed tentative identification of another new complex, $Ru(III)Cl_3(PCy_3)(bipy)$ (data not shown). In both cases, addition of bipy resulted in an upfield shift of the phosphine peak from 108.10 ppm (activated **1** and activated **3**) to 49.80 ppm (Figures S4 and S8). Moreover, during an attempt to obtain an X-ray crystal structure of activated **3**, we instead isolated and characterized the SIPr·HCl salt. In a separate experiment, when **3** was exposed to ethyl α-bromoisobutyrate in C_6D_6 (Figure 1c), we were able to obtain colorless crystal from this reaction mixture, which turned out to be the SIPr·HBr salt. Both of these results suggest that the NHC ligands are labile under these reaction conditions.

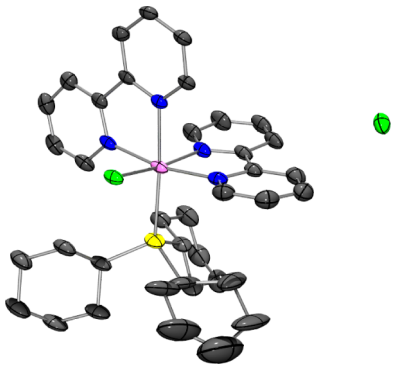

Figure 3. X-ray crystal structure of $Ru(II)Cl(PCy_3)(bipy)_2Cl^-$ formed from addition of bipy to ATRA-activated **1**. Hydrogen atoms and solvent molecules were omitted for clarity. Pink, Ru; gray, C; yellow, P; blue, N; green, Cl (CCDC 1473173).

Combining the insights from all of these experiments, we now suspect that the original ruthenium benzylidene complexes decompose under common ATRA reaction condition (65 °C in $CHCl_3$) through complete dissociation of all L-type ligands (benzylidene, PCy_3, and NHC) from the ruthenium metal center. We propose that a simple ruthenium chloride complex, such as $Ru(III)Cl_3$ or $Ru(II)Cl_2$ or a Ru_xCl_y cluster, possibly containing one or more bound phosphine ligands, is the actual ATRA-active species. To explore this possibility further, we attempted to perform ATRA with $Ru(III)Cl_3$, which we found to be completely insoluble in $CHCl_3$ even upon addition of MMA. To solubilize this complex, $Ru(III)Cl_3$ was refluxed with PCy_3 in MeOH overnight, concentrated in vacuo, suspended in benzene, filtered, washed with benzene and dried. The resulting ruthenium complex, presumably $RuCl_3(PCy_3)_n$, was soluble in $CHCl_3$ and successfully converted MMA to the ATRA product with 96% MMA conversion and 88% product yield (Figure S14). Also, the reaction kinetics with $RuCl_3(PCy_3)_n$ were faster than with **3** and were in perfect agreement with ATRA-activated **3**. The newly prepared $RuCl_3(PCy_3)_n$ complex, however, did not show the same peaks in the ^{31}P spectrum as activated **1** or activated **3** (108.10 ppm). This experiment confirms that the phosphine peak from 108.10 ppm in ATRA-activated **3** is a byproduct from the catalyst activation process and does not correspond to a ruthenium species that is involved in ATRA reactions.

Lastly, we performed a series of experiments to test whether insights gained from this investigation were relevant to ATRP. ATRP and ATRA have similar mechanisms involving active radicals generated by a reversible redox process of halogenated substrates and transition metal complexes.[28] In ATRP, a large excess of olefin leads to polymerization rather than a single radical addition. Ruthenium benzylidene complexes **1**–**5** converted MMA to polymer (Scheme 3, Figure 4). The

Scheme 3. ATRP of MMA Catalyzed by Ruthenium Benzylidenes

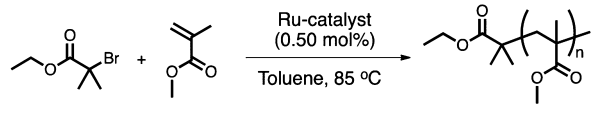

11 MMA 12

[**11**] : [MMA] : [catalyst] = 1 : 200 : 1

0.02 M **11** in toluene

order of reaction rates was similar to the previous catalytic ATRA, except that **4** was the slowest in ATRP. However, only **1** and **3** polymerized MMA in a controlled fashion to yield polymers with linear molecular weight increases and low dispersities. Polymerization with **2**, **4**, and **5** showed constant molecular weight, indicating early termination of the polymer chains and even undesired coupling reactions in the case of **5**. It has been reported that some ruthenium benzylidenes preferentially promote redox-initiated free radical polymer-

DOI: 10.1021/jacs.6b03767
J. Am. Chem. Soc. 2016, 138, 7171−7177

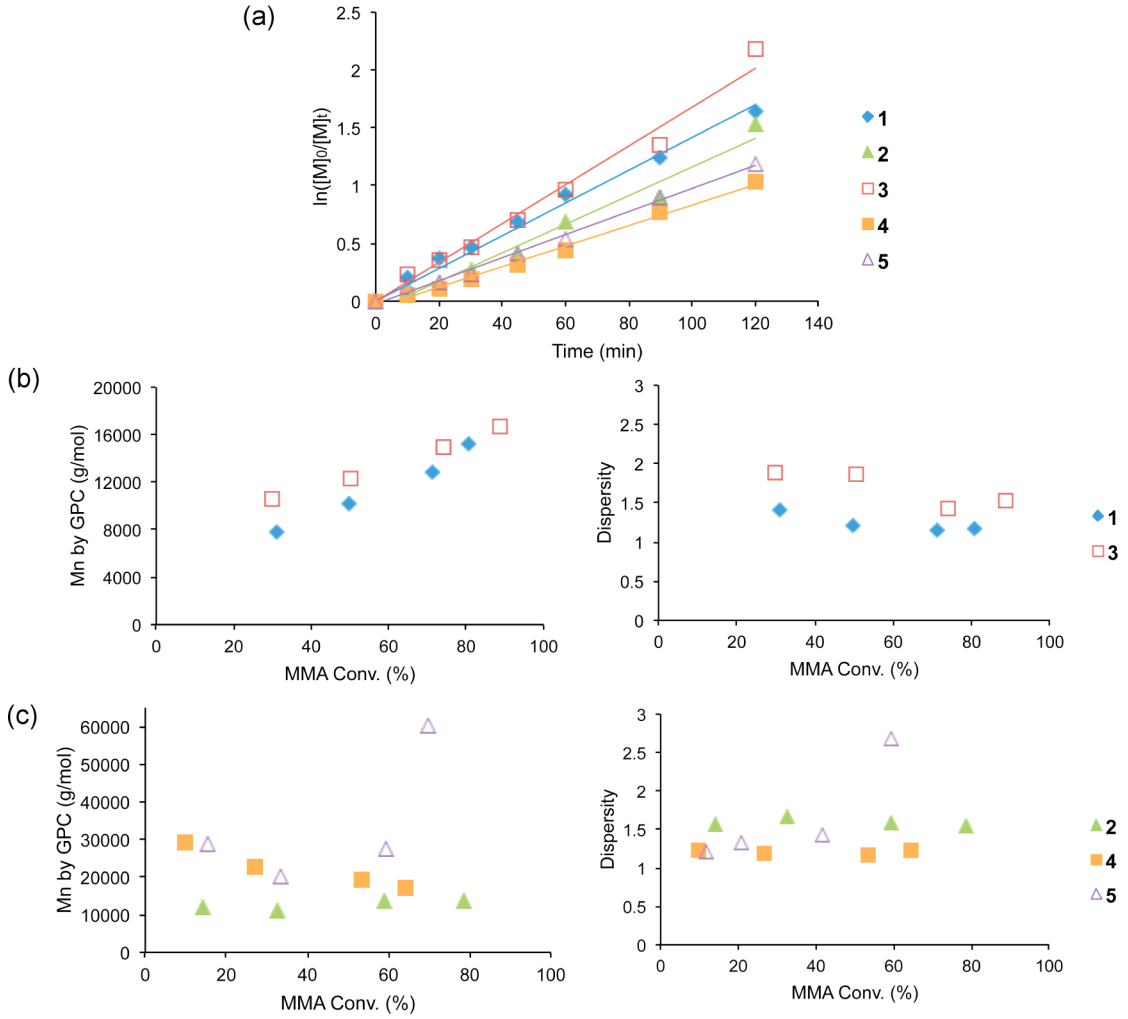

Figure 4. Kinetic studies of ATRP catalyzed by ruthenium benzylidene complexes. (a) $\ln([M]_0/[M]_t)$ over time. (b) M_n and $Đ$ over MMA conversion with **1** and **3**. (c) M_n and $Đ$ over MMA conversion with **2**, **4**, and **5**.

ization over ATRP;[18] however, no clear explanation has been put forward to rationalize the differences. The present work shows that complexes **1** and **3**, which exhibited rapid in situ conversion in $CHCl_3$ with high product yield in ATRA, also promoted efficient ATRP. A well-known side reaction of ATRA is polymerization/oligomerization, which can proceed via redox-initiated free radical polymerization. Thus, the ATRA data can be used to explain which ruthenium benzylidene precatalysts favors ATRP over free radical polymerization.

CONCLUSION

We have discovered that, under ATRA conditions, ruthenium benzylidene complexes are transformed into one or more new ATRA-active, metathesis-inactive ruthenium species, possibly a simple $Ru_xCl_y(PCy_3)_z$ complex. The same complexes that give high yields and minimal competing side reactions in ATRA also promote living ATRP over uncontrolled free radical polymerization. The results of this study showcase the importance of mechanistic inquiry as a means of better understanding and ultimately improving tandem catalytic reactions.

ASSOCIATED CONTENT

Supporting Information

The Supporting Information is available free of charge on the ACS Publications website at DOI: 10.1021/jacs.6b03767.

All of the detailed experimental procedures, NMR spectra, and computational data (PDF)

Crystal data (CIF)

AUTHOR INFORMATION

Corresponding Author

*rhg@caltech.edu

Present Address

§K.M.E.: The Scripps Research Institute, Department of Chemistry, 10550 N. Torrey Pines Rd., La Jolla, CA 92037.

Notes

The authors declare no competing financial interest.

ACKNOWLEDGMENTS

The research described was financially supported by the ONR (Award N00014-12-1-0596) and the NIH NIGMS (Award F32GM108145; postdoctoral fellowship to K.M.E.). The authors thank Materia, Inc. for generous donation of catalysts **1**, **2**, **3**, **6**, and **7**. The authors also thank Dr. Michael Haibach (Grubbs group, Caltech), Dr. Peter Dornan (Grubbs group, Caltech), and Dr. Buck L. H. Taylor (Houk group, UCLA) for the helpful discussions. Calculations were performed using the NSF funded (OCI-1053575) Extreme Science and Engineering

DOI: 10.1021/jacs.6b03767
J. Am. Chem. Soc. 2016, 138, 7171−7177

Discovery Environment (XSEDE) and the UCLA Hoffman2 Cluster.

REFERENCES

(1) Matsumoto, H.; Nakano, T.; Nagai, Y. *Tetrahedron Lett.* **1973**, *14*, 5147−5150.
(2) Ando, T.; Kamigaito, M.; Sawamoto, M. *Tetrahedron* **1997**, *53*, 15445−15457.
(3) Simal, F.; Wlodarczak, L.; Demonceau, A.; Noels, A. F. *Tetrahedron Lett.* **2000**, *41*, 6071−6074.
(4) Simal, F.; Sebille, S.; Demonceau, A.; Noels, A. F.; Nuñez, R.; Abad, M.; Teixidor, F.; Viñas, C. *Tetrahedron Lett.* **2000**, *41*, 5347−5351.
(5) Simal, F.; Wlodarczak, L.; Demonceau, A.; Noels, A. F. *Eur. J. Org. Chem.* **2001**, 2689−2695.
(6) Tutusaus, O.; Delfosse, S.; Demonceau, A.; Noels, A. F.; Viñas, C.; Teixidor, F. *Tetrahedron Lett.* **2003**, *44*, 8421−8425.
(7) Kato, M.; Kamigaito, M.; Sawamoto, M.; Higashimura, T. *Macromolecules* **1995**, *28*, 1721−1723.
(8) Kamigaito, M.; Ando, T.; Sawamoto, M. *Chem. Rev.* **2001**, *101*, 3689−3746.
(9) Simal, F.; Demonceau, A.; Noels, A. F. *Angew. Chem., Int. Ed.* **1999**, *38*, 538−540.
(10) Matyjaszewski, K.; Xia, J. *Chem. Rev.* **2001**, *101*, 2921−2990.
(11) Simal, F.; Jan, D.; Delaude, L.; Demonceau, A.; Spirlet, M.-R.; Noels, A. F. *Can. J. Chem.* **2001**, *79*, 529−535.
(12) Kamigaito, M.; Watanabe, Y.; Ando, T.; Sawamoto, M. *J. Am. Chem. Soc.* **2002**, *124*, 9994−9995.
(13) Opstal, T.; Verpoort, F. *New J. Chem.* **2003**, *27*, 257−262.
(14) Camerano, J. A.; Rodrigues, A.-S.; Rominger, F.; Wadepohl, H.; Gade, L. H. *J. Organomet. Chem.* **2011**, *696*, 1425−1431.
(15) Faulkner, J.; Edlin, C. D.; Fengas, D.; Preece, I.; Quayle, P.; Richards, S. N. *Tetrahedron Lett.* **2005**, *46*, 2381−2385.
(16) Lee, B. T.; Schrader, T. O.; Martín-Matute, B.; Kauffman, C. R.; Zhang, P.; Snapper, M. L. *Tetrahedron* **2004**, *60*, 7391−7396.
(17) Simal, F.; Demonceau, A.; Noels, A. F. *Tetrahedron Lett.* **1999**, *40*, 5689−5693.
(18) Simal, F.; Delfosse, S.; Demonceau, A.; Noels, A. F.; Denk, K.; Kohl, F. I.; Weskamp, T.; Herrmann, W. A. *Chem. - Eur. J.* **2002**, *8*, 3047−3052.
(19) Tallarico, J. A.; Malnick, L. M.; Snapper, M. L. *J. Org. Chem.* **1999**, *64*, 344−345.
(20) Bielawski, C. W.; Louie, J.; Grubbs, R. H. *J. Am. Chem. Soc.* **2000**, *122*, 12872−12873.
(21) Seigal, B. A.; Fajardo, C.; Snapper, M. L. *J. Am. Chem. Soc.* **2005**, *127*, 16329−16332.
(22) Borguet, Y.; Sauvage, X.; Zaragoza, G.; Demonceau, A.; Delaude, L. *Beilstein J. Org. Chem.* **2010**, *6*, 1167−1173.
(23) Fogg, D. E.; dos Santos, E. N. *Coord. Chem. Rev.* **2004**, *248*, 2365−2379.
(24) Sanford, M. S.; Love, J. A.; Grubbs, R. H. *Organometallics* **2001**, *20*, 5314−5318.
(25) Leitao, E. M.; Piers, W. E.; Parvez, M. *Can. J. Chem.* **2013**, *91*, 935−942.
(26) Ritter, T.; Hejl, A.; Wenzel, A. G.; Funk, T. W.; Grubbs, R. H. *Organometallics* **2006**, *25*, 5740−5745.
(27) Shih, W.-C.; Ozerov, O. V. *Organometallics* **2015**, *34*, 4591−4597.
(28) Richel, A.; Delfosse, S.; Cremasco, C.; Delaude, L.; Demonceau, A.; Noels, A. F. *Tetrahedron Lett.* **2003**, *44*, 6011−6015.

DOI: 10.1021/jacs.6b03767
J. Am. Chem. Soc. 2016, 138, 7171−7177